GEOPHYSICAL RESEARCH LETTERS, VOL. 23, NO. 3, PAGES 233-236, FEBRUARY 1, 1996

Seismicity and stress-drop in the eastern Transverse ranges, Southern California

Laura E. Jones and Donald V. Helmberger
Seismological Laboratory, California Institute of Technology, Pasadena

Abstract. Stress–drops for small to moderately sized earthquakes in Southern California are found to vary systematically with source–depth and location (tectonic environment). We determine high–quality fault–plane solutions, plus depth and source duration, for 17 significant ($M > 3.9$) aftershocks associated with the June 28, 1992 Big Bear sequence, including the more recent April 4, 1994 19:04 GMT M_w 4.6 Lake Arrowhead aftershock, and a M_w 4.2 Banning Pass event which occurred on May 31, 1993 at 08:55 GMT. Given source durations and moments obtained from long–period source estimations, and assuming a circular fault model, we estimate stress–drop for each event. Big Bear aftershocks are moderate to high (> 100 bars) stress–drop. Events deeper than 12 km are generally high stress–drop (> 100 bars), while shallower events exhibit moderate to high stress–drops. These results are compared with a similar analysis of Landers aftershocks in the Mojave block. For the Big Bear region, stress drops appear to correlate with depth, with the deepest events yielding the highest stress-drops. In general, events in this region yield higher stress-drops than events occuring in the Mojave block and those associated with the Landers and Joshua Tree sequences. Comparisons of M_L to M_o are consistent with the stress–drop results: deep, high stress–drop events show elevated M_L to M_o ratios.

Introduction

The M_w 6.5 1992 Big Bear, Southern California mainshock and its aftershock sequence appears to have occurred almost entirely within the San Bernardino Mountains block [Hauksson et al., 1993; Jones and Hough, 1995]. The Big Bear mainshock was the largest of thousands of aftershocks following the M_w 7.3 1992 Landers event. In the aftermath of this complex and enigmatic event and its lengthy and energetic aftershock sequence, we take a second look at seismicity within and bordering the San Bernardino mountains.

Generally high levels of apparent stress (the ratio of radiated energy to moment, see Brune, 1968) have been reported for the San Gorgonio Pass area of the eastern Transverse ranges [Wyss and Brune, 1971]. Our study area includes this region and the San Bernardino Mountains block north thereof. We include depth and fault parameter information in our analysis as well as estimates of source dimension, which allows for correlation of source location, type and depth with level of stress drop. Finally, results from the Mojave region (Joshua Tree, Landers, Barstow sequences), and the eastern Transverse Ranges (Big Bear, Arrowhead, Banning) are compared.

Paper number 96GL00012
0094-8534/96/96GL-00012$03.00

Data and Analysis

The earthquakes examined in this study were recorded on the broadband instruments of TERRAscope array, which is in the process of ongoing enlargement. Thus, events recorded in 1992 were recorded at the six stations GSC, ISA, PAS, PFO, SVD, and SBC (we use records from the former five), while events recorded later may include records from stations Needles (NEE), Barrett (BAR), Victorville (VTV). Prior to analysis, instrument gain was removed from the velocity records; they were detrended and integrated once. A butterworth bandpass filter with corners at 0.04 and 7 Hz was applied twice. Filtering was minimal so that the broad-band nature of the records might be preserved.

Average source parameters for the aftershocks considered in this study are estimated using a grid–search algorithm developed by Zhao and Helmberger [1994]. The comparisons are done broadband, and using broadband data convolved with a long–period instrument response [Figure 1]. The long–period filter is applied to minimize data–model misfit and produce a stable solution from a small data set which might otherwise contain difficult to model high–frequency information. Long–period data thus obtained are less sensitive to source duration, however, so broadband data and data convolved with a short–period instrument response are used for the estimation of appropriate source–time functions.

Source depths are determined directly from the surface reflected phases sP_mP or sS_mS, or estimated by cycling through depth–dependent Green's functions (2, 5, 8, 11, 14, and 17 km) to obtain an average depth for the event. We employ a catalog of Green's functions appropriate to the standard Southern California model [Dreger and Helmberger, 1991ab] which are computed at 5 km intervals from 35 km to 400 km, using the reflectivity method.

Source duration and stress–drop

Effective source–time functions are determined for each event both by direct search (i.e., by seeking a best–fit source–duration) and by doing a simple comparison of energies. Estimation of source–duration by comparison of short–period to long–period energy content provides a robust and easily automated way of obtaining durations, unlike the former trial–and–error method. For this scheme, P_{nl} waves from each station are compared with synthetic P_{nl} waveforms as follows:

$$Ratio = \frac{E_{(obs)}}{E_{(syn)}}$$

where

$$E = \frac{\int_{t_{pn}}^{t_{sn}} [V_{(sp)}]^2 dt}{\int_{t_{pn}}^{t_{sn}} [V_{(lp)}]^2 dt}$$

$V_{(sp)}$ is the observed (or synthetic) P_{nl} wave, in velocity, convolved with a short-period Wood–Anderson response, while $V_{(lp)}$ is the

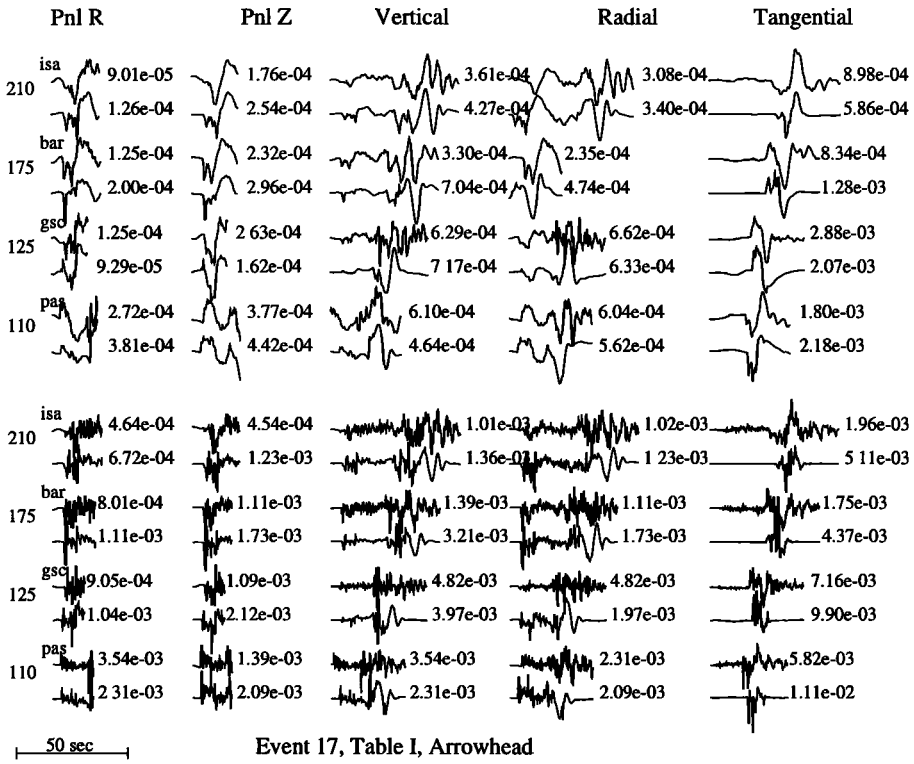

Figure 1. Long–period (top) and Broadband (bottom) waveform modeling for the $M4.6$ April 6, 1994, Arrowhead earthquake. The moment for the long–period (LP3090) solution is $M_o = 8.57 \times 10^{22}$, and for the broadband solution, $M_b = 1.04 \times 10^{23}$. The time function is (0.19, 0, 0.19) s.

observed (or synthetic) P_{nl} wave, in velocity, convolved with a long–period Press–Ewing (LP3090) instrument response. Given the relatively small events, most of which have very short source durations, it is necessary to use the data broadband, or filtered for short–period energy. An example of such an event is shown in Figure 1 (bottom panel). For the synthetics,

$$V = M_o s(t) * A_i(\theta, \lambda, \delta) * G(t, r)$$

where M_o is seismic moment (average for all stations used) $G(t, r)$ is the propagational Green's function, assuming a point source, and $A_i(\theta, \lambda, \delta)$ contains the source radiation pattern. We seek an effective source–time function, $s(t)$, such that $Ratio \sim 1$, by cycling through simple triangles and selecting the appropriate source duration. Durations estimated for each station are then averaged to yield an event duration.

This procedure gives a conservative estimate of source duration and thus stress-drop, and is limited to source triangles no shorter than 0.20 s in duration. This limitation is imposed by the computational technique used and by the frequency content available in the synthetic Green's functions.

Assuming little or no attenuation, the width of the observed P or S pulse is proportional to the source dimension, and thus source duration. The actual pulse-width, as observed, depends on factors as diverse as crustal attenuation, rupture mode, length and velocity, and source complexity. On average, however, it is acceptable to assume a linear relationship between pulse–width and source dimension. Cohn et al. [1982], assuming a circular fault [Brune, 1970], obtained the relation

$$\tau = \frac{2.62a}{\beta}$$

where τ is the source duration in seconds, a is the radius in km, and β is the shear velocity local to the source region. Solving for a in terms of τ, assuming a shear velocity of 3.5 km/s, and substituting the result into the expression for stress–drop on a circular fault, we obtain

$$\triangle\sigma = \frac{1.84 \times 10^{-22} M_o}{\tau^3}$$

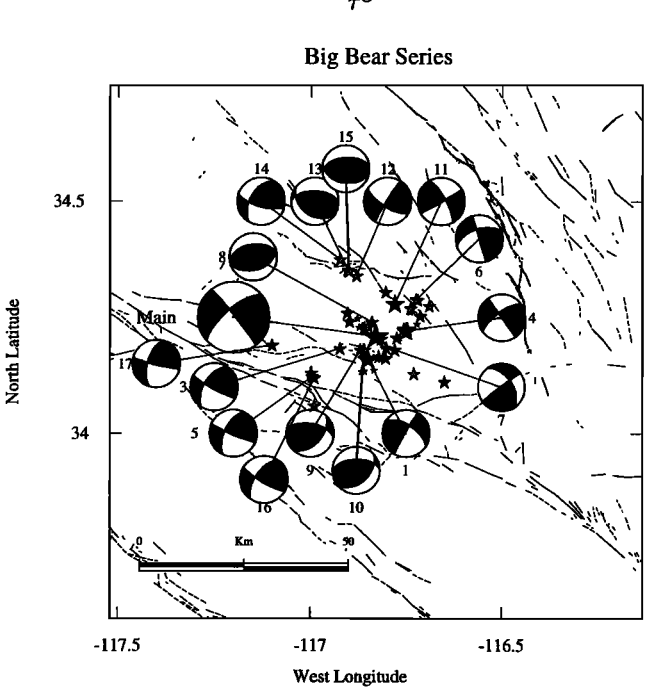

Figure 2. Map showing locations of the Big Bear earthquake (large star) and $M > 1.9$ aftershocks in the sequence (smaller stars). Events with focal spheres are numbered in the order of occurrence, and listed in the same order [Table I].

For our purposes, stress drops are depicted on plots of moment versus duration.

Seismicity and stress-drop in the Big Bear region

Seismicity associated with the Big Bear sequence appears to have occurred almost entirely within the San Bernardino Mountains block [Jones and Hough, 1995]. The sequence is dominated by deep to intermediate depth NW-striking right-lateral and NE-striking left-lateral strike-slip events on trends parallel to both planes of the mainshock source mechanism. Primarily strike-slip earthquakes (presumably left-lateral, from their alignment) lie along or form trends parallel to the broad northeast trending swath of seismicity seen in Figure 2, while right-lateral (again from alignment) and thrust events tend to lie along northwest trends, and along the northern and southwestern ends of the aftershock trends. Deep events yield the highest stress-drops, even for smaller earthquakes [Table 1, Figures 2 and 3].

Aftershocks along the North Frontal fault (Figure 2, Table 1, events 6, 11, 12, 13, 14, 15) tend to have low to moderate stress-drops, averaging about 55 bars. Event 12 is the largest of these events, with magnitude M_w 5.2, and a stress-drop of 112 bars, unusually high for a shallow event in this region. North-frontal fault aftershocks also tend to be moderate to shallow in depth, while those just south of the mainshock are deep. Furthermore, events south of the mainshock, including the 14:43 GMT foreshock (Figure 2, Table 1, events 1 and 7) and near the Santa Ana Thrust (Figure 2, Table 1, events 3, 9, 10, and 17) are higher stress-drop, with an average of about 180 bars. Thus there is an apparent shallowing of *larger* aftershocks from south to north within the San Bernardino mountains block, with deep, relatively high stress-drop events south of the Big Bear mainshock, and shallower, moderate to low stress-drop events north of the mainshock [Figure 3].

Prior to the Big Bear mainshock, seismicity in the San Gorgonio-Banning Pass region occurred almost exclusively on the Mill Creek Fault; thereafter, seismicity shifted to other faults, perhaps due to static stress changes caused by the nearby Big Bear mainshock [Seeber and Armbruster, 1995]. We examine two events on the Mill-Creek fault (Figure 2, Table I, events 5 and 16) and compare these with a more recent event which occurred near the Santa Ana Thrust in the vicinity of Lake Arrowhead (Figure 2, Table I, event 17). The prior two events lie within a tight cluster (Yucaipa cluster) which began to form shortly after the Big Bear mainshock. Both are strike-slip events (presumably right-lateral and parallel to the trend of the Mill-Creek fault in that area), of moderate (7-11 km) depth and stress-drop (73 and 33 bars).

In contrast, the "Arrowhead" event (event 17) occurred in a region not previously noted for its activity, was high stress-drop (about 250 bars), and deeper, with an estimated source-depth of 14 km, though its source mechanism is similar to those of the earlier events located on the Mill-Creek fault. Broadband waveform modeling for this event documents its high stress-drop nature: with a magnitude of 1.04×10^{23}, it has an average source duration of only about 0.38

Table 1. Big Bear Events

No.	M_w	strike	dip	rake	depth	τ^a	$\Delta\sigma^b$
1.	5.2	210	86	330	14	0.85	285
(main)	6.5	320	86	200	~14		
3.	4.8	118	83	145	14	0.65	115
4.	4.3	324	90	200	8	0.60	44
5.	4.4	113	85	150	7	0.70	73
6.	4.0	343	90	214	6	0.35	64
7.	3.9	230	80	150	16	0.20	140
8.	5.3	246	46	102	2	1.50	60
9.	4.8	285	65	150	15	0.60	205
10.	4.0	268	52	118	11	0.40	58
11.	4.0	330	75	178	8	0.50	35
12.	5.2	118	70	176	5	1.10	112
13.	5.1	126	43	117	7	1.10	68
14.	4.3	106	72	140	5	0.65	34
15.	4.2	100	40	102	8	0.65	18
16.	4.2	118	78	152	11	0.50	33
17.	4.6	104	86	150	14	0.40	250

[a] source duration in s
[b] stress drop in bars

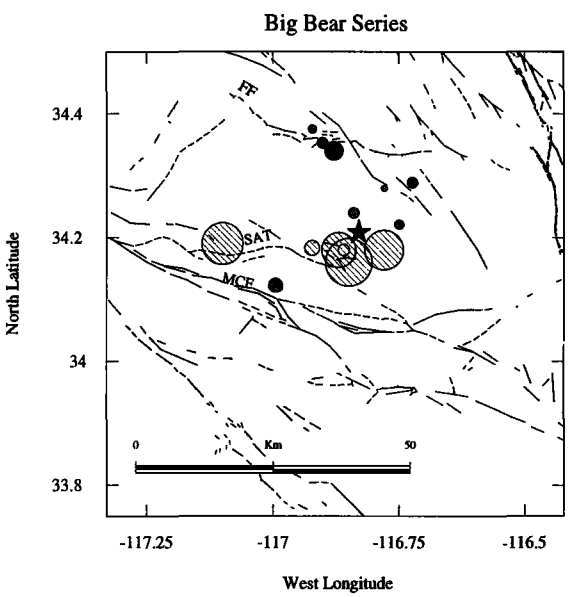

Figure 3. Map showing locations and stress-drops for Big Bear, Yucaipa and Arrowhead events. Deep events are hatched; shallow events and events of moderate depth are shown filled. Stress-drop circles are scaled to a maximum of 280 bars. The Big Bear mainshock is indicated by a filled (black) star. Note the correspondence between deeper epicenters (hatched) and high stress-drop. Faults are labled as follows: FF, North Frontal fault; SAT, Santa Ana thrust; MCF, Mission Creek fault.

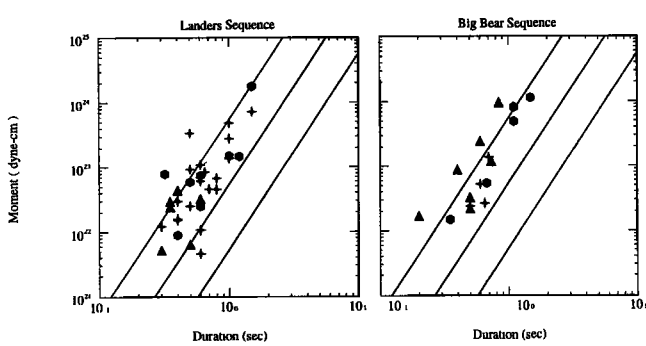

Figure 4. Moments versus durations for Big Bear and Landers aftershocks. Event depths are indicated by different symbols: filled triangles indicate "deep" events (12 to 17 km); filled crosses "intermediate" events (8 to 11 km); and filled hexagons "shallow" events (2 to 7 km). Lines of constant stress drop are plotted diagonally; from bottom to top: 1, 10, and 100 bars.

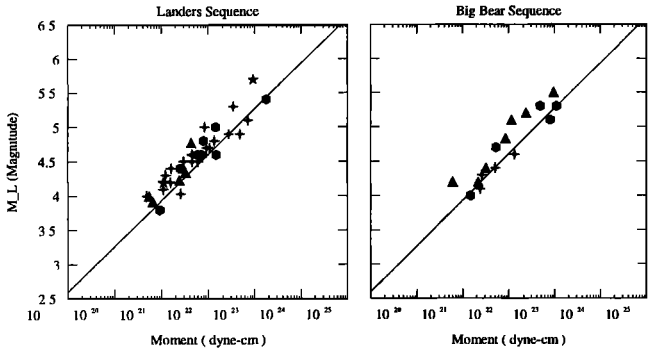

Figure 5. Local magnitudes versus moments for Landers and Big Bear events in Southern California. Symbols indicate depth as in Figure 4. The straight line represents the relation: $M_L = (logM_o - 16.5)/1.5$ [Thatcher and Hanks, 1973]

s [Figure 1]. It is of similar depth (and mechanism), to an event near the Santa Ana Thrust located due west of it (event 3) which occurred within an hour of the mainshock and was classified as a Big Bear aftershock due to mainshock proximity. Though separated by several years, both events are deep and high stress-drop, which suggests that deep, energetic earthquakes are not unusual within the San Bernardinos.

Discussion

Although the exact relationship between stress-drop and regional tectonic stresses is poorly understood, relative stress drop is a meaningful parameter by which to compare various tectonic provinces. For Big Bear, stress–drop increases with increasing depth. Unlike the Landers aftershocks we examined in a similar study [Jones and Helmberger, in preparation, 1995], larger Big Bear quakes are primarily deep. Of 17 Big Bear events studied, 8 are 11 km or deeper. In contrast, of the 36 Landers events studied, only 6 are 11 km or deeper. Furthermore, events occurring in the Big Bear/San Gorgonio Pass regions are generally higher stress–drop than events occurring in the Mojave [Figure 4].

In addition, we compare seismic moments obtained in this study with local magnitudes (M_L) determined from SCSN short–period network data. M_L is more a measure of short–period energy, as the dominant frequency for the determination of local magnitude from this network is about 1 Hz, while the M_o are computed with broadband data convolved with an LP3090 instrument response, which has a dominant frequency of about 0.25 Hz. Note the consistency between the Landers and Big Bear series [Figure 5]; both plot on average just above the relation found by Thatcher and Hanks [1973]. Note also for Big Bear events that high ratios of M_L to M_o correlate well with deep and high stress–drop events [Figure 5]. Landers and Big Bear events are all moderately high stress–drop, (on average about 50 bars for Landers events; 100 bars for Big Bear). Small, high stress-drop events would contain relatively more high frequency energy, which might explain the elevated M_L : M_o ratios.

High stress–drops have been reported for other events near the Transverse Ranges: the 1987 Whittier Narrows event (750 bars, Bent and Helmberger, 1989), the 1990 Upland event (265 bars, Dreger and Helmberger, 1991) and the 1991 Sierra Madre quake (460 bars, Dreger and Helmberger, 1992) are all recent examples. High stress–drops for events in the western transverse ranges are thus more the norm than the exception, and this phenomenon appears to continue eastward into the San Bernardino mountains block.

We propose several explanations for this observation. High stress–drops have been associated with long earthquake reccurrance times [Kanamori and Allen, 1986; Scholz et al., 1986], which could themselves be related to low slip rates on youthful or discontinuous faults. Unusually high stress–drop aftershocks were associated with a nascent fault (the Landers-Kickapoo fault, [Spotila and Sieh, 1995; Jones and Helmberger, in preparation, 1995]) during the Landers sequence. It is thus plausible that high stress–drop events in the central and eastern transverse ranges are similarly associated with immature or discontinuous faults in a tectonically complex region. Direct seismological evidence of the region's complexity is provided by the heterogeneity of the Big Bear aftershock sequence itself, as well as the complexity of the Big Bear mainshock [Jones and Hough, 1995], which may have ruptured on conjugate fault planes.

Acknowledgments. This research was supported by USGS grant 1434-94-G2322. Contribution number 5573, Division of Geological and Planetary Sciences, California Institute of Technology, Pasadena, CA 91125.

References

Brune, J. N., Seismic Moment, seismicity and rate of slip along major fault zones, *J. Geophys. Res., 73*, 777-784, 1968.

Brune, J.N., Tectonic stress and the spectra of seismic shear waves from earthquakes, *J. Geophys. Res. 75*, 4997–5009, 1970.

Cohn, S. N., T. L. Hong and D. V. Helmberger, The Oroville earthquakes: a study of source characteristics and site effects, *J. Geophys. Res., 87*, 4585–4594, 1982.

Dreger, D. S., and Helmberger, D.V., Complex faulting deduced from broadband modeling of the 28 february 1990 Upland earthquake ($M_L = 5.2$), *Bull. Seism. Soc. Am., 81* 1129–1144, 1991.

Dreger, D. S., and Helmberger, D. V., Source Parameters of the Sierra Madre Earthquake from regional and local body waves, *Geophys. Res. Lett., 18*, 2015-2018, 1991.

Hauksson, E., L. M. Jones, K. Hutton and D. Eberhart-Phillips, The 1992 Landers Earthquake Sequence: Seismological Observations, *J. Geophys. Res., 98*, 19,835–19,858, 1993.

Jones, L. E., and S. E. Hough, Analysis of Broadband Records from the 28 June 1992 Big Bear Earthquake: Evidence of a Multiple–Event Source, *Bull. Seism. Soc. Am.*, 85, 688–704, 1995.

Kanamori, H., and Allen, C. A., Earthquake repeat time and average stress–drop, **Earthquake Source Mechanics**, Geophys. Monograph 37, AGU, 227–235, 1986.

Scholz, C. H., C. A. Aviles, S. G. Wesnousky, Scaling differences between large and intraplate earthquakes, *Bull. Seism. Soc. Am., 76*, 65-71, 1986.

Seeber, L. and J. G. Armbruster, The San Andreas Fault system throught the Transverse Ranges as illuminated by earthquakes, *J. Geophys. Res.*, in press, 1995.

Thatcher, W., and Hanks, T. C., Source Parameters of Southern California Earthquakes, *J. Geophys. Res., 78*, 8547–8576, 1973.

Wyss, M. and J. N. Brune, Regional Variations in source properties in southern California estimated from the ratio of short– to long–period amplitudes, *Bull. Seism. Soc. Am., 61*, 1153–1168, 1971.

Zhao L–S., and D. V. Helmberger, Source Estimation from Broadband Regional Seismograms, *Bull. Seism. Soc. Am., 84*, 91-104, 1994.

Laura E. Jones, Seismological Laboratory, California Institute of Technology 252-21, Pasadena, CA 91125.

Donald V. Helmberger, Seismological Laboratory, California Institute of Technology 252-21, Pasadena, 91125.

(received July 24, 1995; accepted September 7, 1995.)